Formation of GaAsN nanoinsertions in a GaN matrix by metal-organic chemical vapour deposition

**A F Tsatsul'nikov†, I L Krestnikov†, W V Lundin†, A V Sakharov†,
A P Kartashova†, A S Usikov†, Zh I Alferov†, N N Ledentsov‡,
A Strittmatter‡, A Hoffmann‡, D Bimberg‡, I P Soshnikov§,
D Litvinov§, A Rosenauer§, D Gerthsen§ and A Plaut∥**

† Ioffe Physico-Technical Institute of Russian Academy of Sciences, Politekhnicheskaya 26,
194021, St Petersburg, Russia
‡ Technische Universität Berlin, Hardenbergstrasse 36, 10623 Berlin, Germany
§ Universität Karlsruhe, Kaiserstr.12, 76128 Karlsruhe, Germany
∥ Exeter University, Stocker Road, Exeter EX4 4QL, UK

Abstract. Coherent ultrathin GaAsN insertions are formed in a GaN matrix by predeposition
of an ultrathin GaAs layer on a GaN surface, followed by annealing in an NH_3 atmosphere
and overgrowth with GaN. During the overgrowth, most of the As atoms are substituted by N,
with a dense array of coherent GaAsN nanodomains with lateral sizes of about 3–4 nm
formed in the GaN matrix. We report a green luminescence due to GaAsN insertions,
surviving at high observation temperatures and excitation densities.

1. Introduction

The development of (In,Ga)N–(Al,Ga)N heterostructures allowed the creation of efficient light-emitting diodes operating in the green–ultraviolet range [1–6]. This opens up new opportunities in colour displays, diode-pumped luminescent panels, etc. However, despite the band gap of InAlGaN alloys ranging between 1.95 and 6.2 eV at room temperature, lasing is only realized in the UV–blue spectral range. Attempts to shift the laser emission wavelength towards green by increasing the In content have failed because of the severe degradation of the optical properties of the material with increasing lattice mismatch.

An alternative way to shift the emission towards longer wavelengths is to use GaAsN–GaN heterostructures. It has been shown both theoretically and experimentally that the GaAsN alloy is characterized by a very large band-gap bowing parameter and even very small additions of As may strongly decrease the band gap [7–9]. For the GaAs-corner of the GaAs–GaN diagram, this resulted in the creation of high-quality 1.3-μm-emitting lasers on GaAs substrates [10]. One may conclude that use of a similar approach for the GaN-rich corner will furnish even more opportunities to extend the emission range of GaN-based structures, the bowing parameter being larger in this case. Additionally, the hexagonal phases of GaAsN and GaN are calculated to have significantly different lattice constants. It is well established now that the lattice-mismatched epitaxial growth may result in the formation of nanodomains either via islanding at the surface or via spinodal decomposition

of the alloy [11]. The emission range for the same average thickness of a narrow-gap insertion can be extended in this case both owing to the nature of the GaAsN alloy and through formation of nanodomains of the smaller-bandgap phase. At the same time, direct attempts to incorporate GaAs in a GaN matrix [12–14] appear to be not very successful. It was found that phase-separation effects lead to dislocated GaAs clusters in a GaN matrix, rather than to coherent quantum dots, when molecular beam epitaxy is used to produce multiple GaAs insertions in GaN [13]. Direct growth of GaAsN by metal-organic chemical vapour deposition (MOCVD) with arsine and NH_3 failed to provide good results because of the low incorporation probability of arsenic atoms in the NH_3 environment [14]. There have been attempts to fabricate GaAs layers in GaN by using multilayer MOCVD GaN–GaAs deposition; however, no structural characterization has been performed and the main optical properties of the structures remain unclear [14].

In this work, different techniques for As incorporation into MOCVD-grown GaN layers have been investigated. The approach was based on deposition of thin GaAs layers onto the GaN surface with further GaN overgrowth using NH_3. High-resolution transmission electron microscopy (HRTEM) of the samples revealed the formation of GaAsN nanodomains with high density and characteristic lateral size of 3–4 nm, originating at the GaN buffer–GaAs epilayer interface. The arsenic content in the inclusions was up to 32%. Additionally, a pronounced diffusion of excess As atoms towards the substrate was observed. We attribute the

photoluminescence (PL) line lying in the green spectral range (~2.45 eV) to these GaAsN insertions.

2. Experiment

The structures were grown on c-plane sapphire using a low-pressure MOCVD machine with a horizontal-flow reactor. Ammonia and trimethylgallium were used as component precursors. Purified hydrogen served as a carrier gas. Either tertiarybutylarsine (TBAs) or 10% dilution of arsine (AsH$_3$) in hydrogen was used as a source of As. Cross-sectional HRTEM investigations were performed on a PHILIPS CM 200 FEG/ST electron microscope with a Scherzer resolution of 0.24 nm. The PL was excited using a He–Cd laser, with excitation density of 25 W cm^{-2}, and registered with a cooled photomultiplier.

3. Results and discussion

The presumed main obstacles to As incorporation are the significant difference between the optimal substrate temperatures for the MOVPE growth of GaAs (600–750 °C) and GaN (1000–1100 °C) and the fast substitution of As atoms by N in the NH$_3$ ambient. To circumvent the above difficulties, we used an approach based on the deposition of thin GaAs layers with the exposure of GaAs to NH$_3$, followed by GaN overgrowth. In this case, the probability of complete substitution of As atoms is reduced. A similar technique was used in [14]. In this work, thin GaAs layers were deposited and covered with GaN and a conclusion was made that As incorporates as an impurity at very low concentrations. The PL emission near 2.6 eV was observed in the spectral range earlier reported for the PL line in As-implanted GaN epilayers. No HRTEM studies were performed, however, to confirm this conclusion. In our work, we deposited a 60-nm-thick GaAs layer on top of the GaN buffer layer at 730 °C. Then the substrate temperature was raised to 1030 °C under AsH$_3$ flux. After the GaAs surface was exposed to ammonia flux, GaN growth was initiated. The thickness of the cap GaN layer was 0.05 μm.

After the structure was fabricated, secondary-ion mass spectrometry (SIMS) and HRTEM were performed. A SIMS profile of the investigated sample is presented in figure 1. The near-surface region, close to the nominal position of the GaAs–GaN interface, is strongly enriched in As. However, a 400-nm-thick As-doped GaN ([As] ~ 3 × 10^{18} cm^{-3}) layer is also observed. As follows from figure 1, the described growth procedure results, first, in the formation of an As-rich region and, second, in the diffusion of As atoms into the GaN epilayer during annealing/initiation of GaN overgrowth. As a result, a relatively thick As-doped GaN layer is formed.

A cross-sectional TEM image of a GaAsN/GaN heterostructure, taken close to the [1$\bar{1}$00]-zone axes (figure 2), shows no defects, indicating that coherent inclusions are formed in the growth procedure used in this work, as contrasted to [13]. According to the TEM investigations, the density of the threading dislocations in the structure with GaAsN layer is about 2 × 10^9 cm^{-2}. This value is comparable with the dislocation density observed for InGaN–GaN structures used to fabricate light-emitting devices.
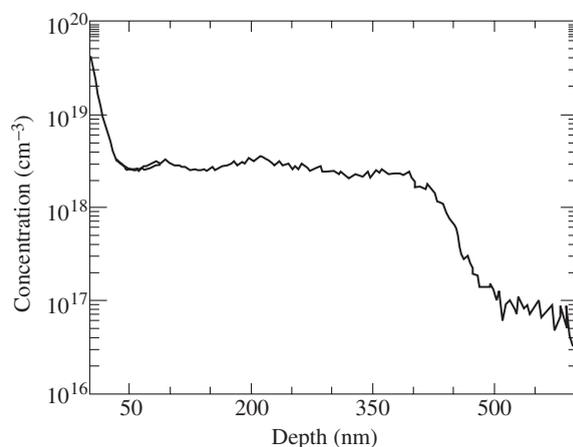

Figure 1. SIMS profile of a sample grown with predeposition of a 60-nm-thick GaAs layer, followed by high-temperature annealing/GaN overgrowth.
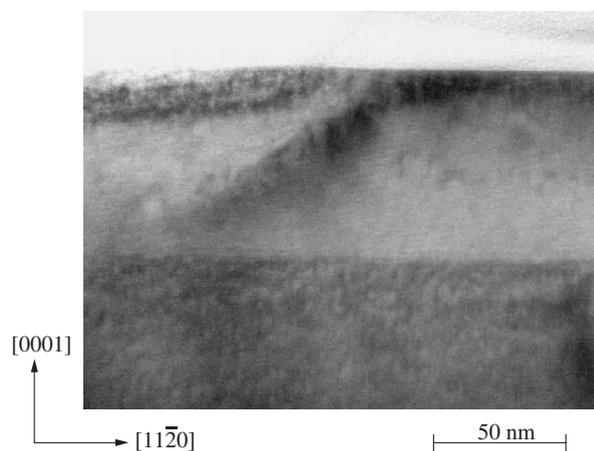

Figure 2. Cross-sectional TEM image of GaAsN/GaN heterostructure taken close to the [1$\bar{1}$00]-zone axes, tilted by about 5° in the [11$\bar{2}$0] direction.

Thus, the insertion of a GaAsN layer does not lead to any dramatic increase in the dislocation density. However, the presence of the dislocations can stimulate diffusion of As atoms and spreading of the As atom distribution, which agrees with the results of SIMS.

To evaluate quantitatively the As concentration profile in the near-surface region of the GaN buffer–GaN cap layer interface, HRTEM studies have been performed. Figure 3(a) shows a HTREM lattice-fringe image of a region of the structure corresponding to the nominal interface region. No extended defects with a [0001] displacement vector, associated with the GaAs predeposition, are observed.

Quantitative information on the As distribution in the GaAs–GaN interface region was obtained by HRTEM image processing. Digitized HRTEM lattice-fringe images were processed using the evaluation program DALI [15]. This program allows a precise measurement of the (0002)-plane distances (LLP: local lattice parameters) correlated with the local composition. The lattice-fringe images were taken with only the (0002) and (000$\bar{2}$) reflections strongly excited, to reduce artifacts induced by thickness variations of the TEM sample [16]. Figure 3(b) displays a colour-coded (shaded
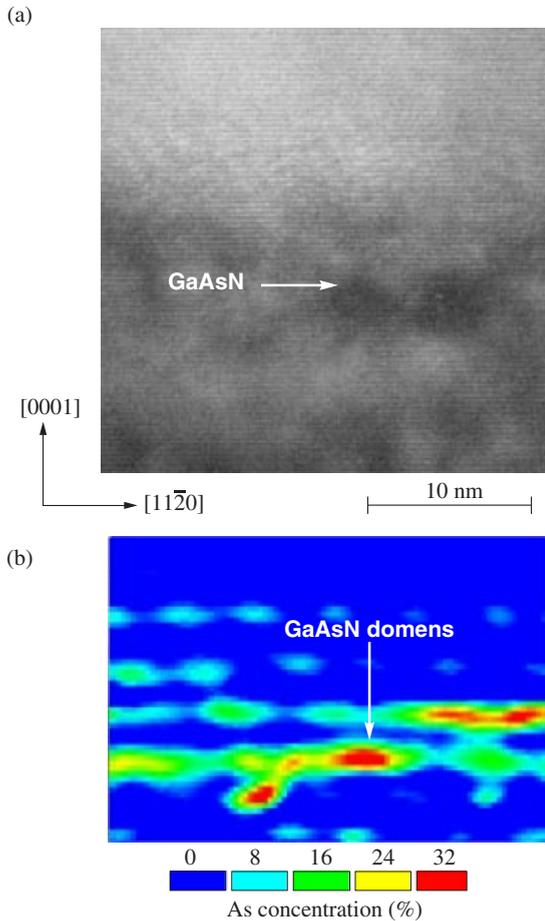
(a)

(b)

Figure 3. (*a*) HRTEM lattice fringe image of the interface GaN-buffer/GaAs/GaN-cap and (*b*) a DALI processed image of the same area.

Figure 4. PL spectrum of a sample with 60-nm-thick GaAs layer. Inset shows the intensity of BL, GL and YL lines as functions of excitation density.

Figure 5. PL spectrum of a thin converted GaAsN layer.

in print version) map of the LLPs converted into local As concentrations. The white regions in figure 3(*b*) denote increased LLPs which correspond to high As concentrations of up to 32%, with the ratio of the lattice constants for the hexagonal and cubic phases of GaAs assumed similar to that for GaN. The effective full width at half maximum of the compositional profile is about 4–5 nm. HRTEM studies also indicate a non-uniform distribution of arsenic and the formation of As-rich nanodomains having a lateral size of about 3–4 nm. Thus, it can be concluded that the proposed procedure results in the formation of both an As-doped region in GaN (via As diffusion) and GaAsN insertions with high As content. Note that the DALI data provide an As concentration distribution averaged along the electron beam direction across the HRTEM foil thickness (∼15 nm). Since the domain size is smaller than the foil thickness, the actual As content in the insertion may be somewhat higher.

The optical properties of the structures have been investigated by photoluminescence spectroscopy. In addition to the near band-edge GaN emission ('band' line (BL)) and the so-called 'yellow' line (YL), attributed to defects in the GaN region, a new PL emission line peaked at 2.45 eV at 77 K (green line (GL)) was observed (see figure 4). The line remained in the spectrum both at low and at room temperature. This peak energy is somewhat different (shifted
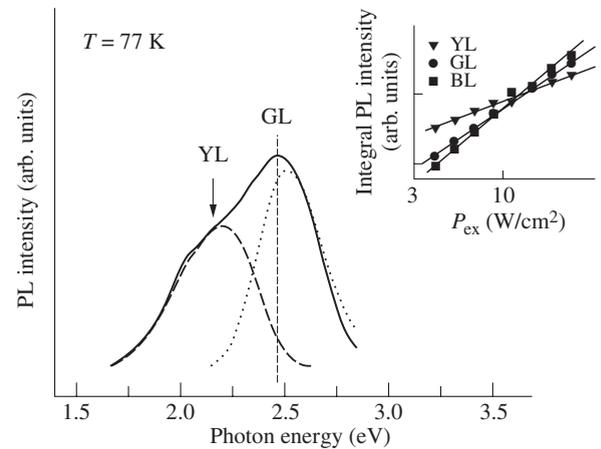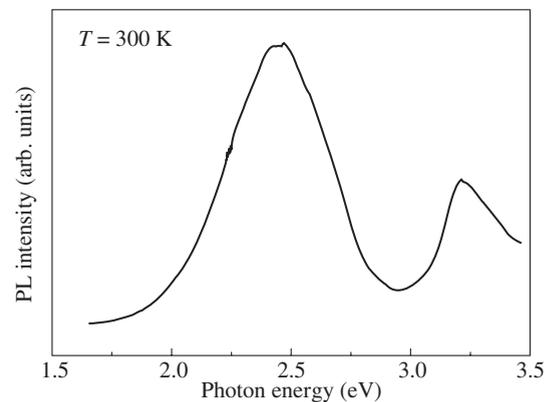
by 150 meV to lower photon energies) from that reported in [14], attributed to As impurities in GaN. The excitation-density dependence of different emission lines is shown in the inset in figure 4. The GL intensity increases superlinearly with excitation density ($I_{GL} \sim I_{ex}^{1.7}$), generally in a way similar to that for the near band-edge luminescence ($I_{BL} \sim I_{ex}^{2}$). GL also remains unsaturated up to excitation densities of about 2 kW cm^{-2}. Also noteworthy is the fact that no GL emission is detected in the PL spectra of the samples grown at low temperatures in the As ambient, using both TBAs and AsH$_3$ [17], when As incorporation is believed to be significant. The GL emission was not observed, either, when a GaAs layer was deposited on a GaN surface and then annealed and evaporated at high temperatures in a hydrogen atmosphere. This process must result in an efficient As diffusion into the GaN layer. In view of both the observations mentioned above, the emission at 2.45 eV does not seem to have As-impurity origin, as it was proposed for 2.6 eV emission in [14]. Thus, the results of the optical studies are in favour of the intrinsic nature of the GL emission. In view of the aforesaid, we believe that the GaAsN nanodomains revealed in the HRTEM studies may be responsible for the emission observed.

To investigate directly the possibility of GaAsN alloy formation during the GaAs–GaN substitution process, we

annealed a GaAs (111) substrate in a nitrogen atmosphere under simultaneous fluxes of arsine and ammonia. The annealing temperature was 1000 °C; the time of annealing, 1 min; arsine and ammonia fluxes were 0.5 slm and 1.7 slm, respectively. This process results in As–N exchange reactions and the conversion of the near-surface GaAs layer into a polycrystalline GaN film composed of hexagonal GaN crystallites with the c-axis perpendicular to the surface, separated from the remaining GaAs substrate and suspended on GaAs needles. For this sample, the GL emission completely dominates the PL spectrum (figure 5). A broad near-band-edge emission from polycrystalline GaN was also observed. Thus, it seems that GaAsN-rich domains can, indeed, be formed during GaAs substitution with GaN. The influence of the As diffusion on the appearance of new Raman lines in GaN epilayers MBE-deposited onto GaAs substrates is discussed in [18].

4. Conclusion

The possibility has been demonstrated of fabricating quantum-dot-like GaAsN insertions in a GaN matrix by the GaAs predeposition–GaN substitution procedure. The size of the QDs is, on the average, smaller than that of QDs formed by ultrathin InGaN insertions. We believe that formation of coherent ultrathin GaAsN nanodomains in a GaN matrix by the proposed process will result in a new way to fabricate GaN–GaAsN and GaN–InGaAsN light-emitting devices operating in an extended wavelength range, similarly to the case of InGaAsN–GaAs devices [10] grown on GaAs substrates.

Acknowledgments

References

[1] Nakamura S, Mukai T and Senoh M 1995 *Appl. Phys. Lett.* **64** 1687

[2] Nakamura S, Senoh M, Iwasa N and Nagahama S 1995 *Appl. Phys. Lett.* **67** 1868

[3] Nakamura S, Senoh M, Iwasa N, Nagahama S, Matsushita T and Mukai T 2000 *Appl. Phys. Lett.* **76** 22

[4] Krestnikov I L, Lundin W V, Sakharov A V, Semenov V A, Usikov A S, Tsatsul'nikov A F, Alferov Zh I, Ledentsov N N, Hoffmann A and Bimberg D 1999 *Appl. Phys. Lett.* **75** 1192

[5] Ledentsov N N, Alferov Zh I, Krestnikov I L, Lundin W V, Sakharov A V, Soshnikov I P, Tsatsul'nikov A F, Bimberg D and Hoffmann A 1999 *Compound Semiconductor* **5** (9), 61

[6] Someya T, Werner R, Forchel A, Catalano M, Cingolani R and Arakawa Y 1999 *Compound Semiconductor* **5** (9), 58

[7] Bellaiche L, Wei S-H and Zunger A 1997 *Appl. Phys. Lett.* **70** 3558

[8] Bi W G and Tu C W 1997 *Appl. Phys. Lett.* **70** 1608

[9] Sakai S, Veta Y and Teauchi Y 1993 *Japan. J. Appl. Phys.* **32** 4413

[10] Egorov A Yu, Bernklau D, Livshits D, Ustinov V, Alferov Zh I and Riechert H 1999 *Electron. Lett.* **35** 1643

[11] Ledentsov N N 1997 *Prog. Cryst. Growth Charact.* **35** 289

[12] Bandi Z Z, Hauenstein R J, O'Steen M L and McGill T C 1996 *Appl. Phys. Lett.* **68** 1510

[13] Goldman R S, Feenstra R M, Briner B C, O'Steen M L and Hauenstein R J 1996 *Appl. Phys. Lett.* **69** 3698

[14] Li X, Kim S, Reuter E E, Bishop S G and Coleman J J 1998 *Appl. Phys. Lett.* **72** 1990

[15] Rosenauer A, Fischer U, Gerthsen D and Forster A 1998 *Ultramicroscopy* **72** 121

[16] Gerthsen D, Hahn E, Neubauer B, Rosenauer A. Schön O, Heuken M and Rizzi A 2000 *Phys. Status Solidi* a **177** at press

[17] Tsatsul'nikov A F, Ber B Ya Kartashova A P, Kudryavtsev Yu A, Ledentsov N N, Lundin V V, Maksimov M V, Sakharov A V, Usikov A S, Alferov Zh I and Hoffmann A 1999 *Semiconductors* **33** (7) 728

[18] Siegle H, Kaschner A, Hoffmann A, Broser I, Thomsen C, Einfeldt S and Hommel D 1998 *Phys. Rev.* B **58** 13619